Sensor-based Planning and Control for Robotic Systems: Introducing Clarity and Perceivability

Devansh R. Agrawal, *Student, IEEE*, Dimitra Panagou, *Senior Member, IEEE*

***Abstract*— In this paper, we first introduce an information measure, termed *clarity*, motivated by information entropy, and show that it has intuitive properties relevant to dynamic coverage control and informative path planning. Clarity defines on a scale of $[0, 1]$ the quality of the information that we have about a variable of interest in an environment. Clarity lower bounds the expected estimation error of any estimator, and is used as the information metric in the notion of *perceivability*, which is defined later on and is the primary contribution of the paper.**

Perceivability captures whether a given robotic (or more generally, sensing and control) system has sufficient sensing and actuation capabilities to gather desired information about an environment. We show that perceivability relates to the reachability of an augmented system, which encompasses the robot dynamics and the clarity about the environment, and we derive the corresponding Hamilton-Jacobi-Bellman equations. Thus, we provide an algorithm to measure an environment's perceivability, and obtain optimal controllers that maximize information gain. In simulations, we demonstrate how clarity is a useful concept for planning trajectories, how perceivability can be determined using reachability analysis, and how a Control Barrier Function controller can be used to design controllers to maintain a desired level of information.

***Index Terms*— Information theory and control; Lyapunov methods; Constrained control**

I. Introduction

ROBOTS are often deployed to explore unknown or unstructured environments, e.g., ocean gliders collecting oceanographic data, or aerial robots searching for targets in a disaster response. In this paper, we establish two concepts: *clarity* and *perceivability*, to capture information acquisition and their use in the design of informative controllers.

Informative Path Planning (IPP) seeks to design trajectories that maximize the 'amount of information' collected subject to budgetary constraints such as total energy or time [1]. 'Information' is measured in many ways, e.g. entropy/mutual information [2]–[5], Fisher Information [6], the number of unexplored cells/frontiers or the area of Voronoi partitions [7]–[10], Gaussian Processes [11], [12], and data-informativity [13]. Various techniques to solve IPP exist, including grid/graph-search or sampling [4], [5], [14], [15]. While useful for trajectory generation, such methods cannot quantify whether information can be gathered in the first place.

This work was supported by the National Science Foundation (NSF) under Grant 1942907. Both authors are at the University of Michigan, Ann Arbor, MI 48109 USA (e-mail: {devansh, dpanagou}@umich.edu).

The main objective is to answer the following questions: *Given a platform (e.g., a robot) with onboard sensors, and an environment in which information is to be collected, (1) does the overall system have sufficient actuation and sensing capabilities to gather information in a specified time, and (2) what are optimal control strategies to collect the information?*

To address these, we first introduce *clarity* as a measure of the quality of information possessed. Clarity about a random variable m, denoted $q[m]$, lies in $[0, 1]$, where $q = 0$ corresponds to the case where m is completely unknown, and $q = 1$ to the case where m is perfectly known in an idealized (noise-free) setting. Clarity is inspired by differential entropy, but compared to the latter it takes finite values with finite time derivatives. As a first contribution, we show that if m is estimated using a Kalman Filter, the rate of change of clarity has a similar structure to one assumed in dynamic coverage controllers [16]–[18]. This establishes certain optimality properties for dynamic coverage control, rather than being viewed as a heuristic for exploration.

The second and primary contribution is the definition of *perceivability*, which quantifies the maximum achievable clarity about the environment in a fixed time by a given system (robot dynamics and sensory outputs). It depends on the controllability of the system describing the robot dynamics, on the observability of the system describing the environment's evolution. This coupling makes perceivability distinct from standard notions of controllability (whether the robot state can be driven to a desired state) or observability (whether the robot state can be uniquely determined from sensory outputs).

We show that perceivability is linked to reachability analysis of an augmented system including both the robot's system dynamics, and the environment's clarity dynamics. We show that perceivability can be determined by solving a Hamilton-Jacobi-Bellman (HJB) equation, which allows us to determine optimal controllers, i.e., those that maximize the quality of information acquired about an environment.

In Sec. II and III we introduce clarity and perceivability, respectively, and in Sec. IV we demonstrate these ideas. Background material is presented where needed.

Notation: $\mathbb{R}, \mathbb{R}_{\geq 0}, \mathbb{R}_{>0}$ are the set of reals, non-negative reals, and positive reals. $\mathbb{S}^n_{++}$, $\mathbb{S}^n_{+}$ denote the set of symmetric positive-definite/positive-semidefinite matrices in $\mathbb{R}^{n\times n}$. $|P|, \operatorname{tr}(P)$ denote the determinant and trace of a square matrix P. $\mathcal{U}(a, b)$ denotes the uniform distribution with support $[a, b] \subset \mathbb{R}^n$. $\mathcal{N}(\mu, \Sigma)$ denotes a normal distribution with mean $\mu \in \mathbb{R}^n$ and covariance $\Sigma \in \mathbb{S}^n_{++}$.

II. Clarity

To aid the reader, we use the following running example, inspired by an oceanographic mission: we wish to create a map of the ocean-surface temperature using sensors onboard a surface vessel, or thermal images from an aerial vehicle, both subject to ocean currents or winds. We require a suitable information metric: for this, we propose clarity.

A. Definitions and Fundamental Properties

Definition 1. [19, Ch. 8] X is a *continuous random variable* if its *cumulative distribution* $F(x) = Pr(X \leq x)$ is continuous. The *probability density function* is $f(x) = F'(x)$. The set where $f(x) > 0$ is the *support set* of X.

Differential entropy extends the notion of entropy [20] from discrete to continuous random variables:

Definition 2. [19, Ch. 8] The *differential entropy* $h[X]$ of a continuous random variable X with density $f(x)$ is

$$h[X] = -\int_S f(x) \log f(x) dx \tag{1}$$

where S is the support set of X.

While differential entropy shares many properties with discrete entropy [19, Sec. 2.1], there are key differences. E.g., while discrete entropy is non-negative, differential entropy is in $[-\infty, \infty]$, i.e., *it can be negative*. We define *clarity* as:

Definition 3. Let X be a n-dimensional continuous random variable with differential entropy $h[X]$. The *clarity* of X is

$$q[X] = \left(1 + \frac{\exp\left(2h[X]\right)}{(2\pi e)^n}\right)^{-1}. \tag{2}$$

The normalizing factor $(2\pi e)^n$ is introduced to simplify some of the algebra, as in Theorem 1 and the next example:

Example 1. Consider $X \sim \mathcal{U}(a, b)$, and $Y \sim \mathcal{N}(\mu, P)$, where $a, b \in \mathbb{R}$, $\mu \in \mathbb{R}^n$, $P \in \mathbb{S}^n_+$. Then,

$$h[X] = \log(b-a), \quad h[Y] = \log\sqrt{(2\pi e)^n |P|},$$
$$q[X] = \frac{1}{1 + \frac{(b-a)^2}{2\pi e}}, \quad q[Y] = \frac{1}{1+|P|}.$$

Next, we establish some fundamental properties of clarity.

Property 1. For any n-dimensional continuous random variable X, $A \in \mathbb{R}^{n\times n}$, and $c \in \mathbb{R}^n$,

$$q[X] \in [0, 1] \qquad \text{(clarity is bounded)} \tag{3}$$
$$q[X + c] = q[X] \qquad \text{(clarity is shift-invariant)} \tag{4}$$
$$q[AX] \neq q[X] \qquad \text{(clarity is } \textit{not} \text{ scale-invariant)} \tag{5}$$

Proof. Of (3)*:* Since $h[X] \in [-\infty, \infty]$, $q[X] = 1/(1+s)$ for some $s \in [0, \infty]$, i.e., $q[X] \in [0, 1]$.

Of (4)*,* (5)*:* Follows from [19, Th. 8.6.3] ($h[X+c] = h[X]$), and [19, Th. 8.6.4] ($h[AX] = h[X] + \log|A|$). □

In information gathering tasks, we seek to design trajectories that minimize the estimation error. Let X be a random variable of *any* distribution with clarity $q[X]$. Let $\hat{X}$ be *any* estimate of X, then $E[(X-\hat{X})(X-\hat{X})^T]$ is the expected estimation error. Theorem 1 shows for expected estimation error to approach 0 it is necessary that clarity approach 1.

Theorem 1. *For any n-dimensional continuous random variable X and any $\hat{X} \in \mathbb{R}^n$, the determinant of the expected estimation error is lower-bounded as*

$$\left|E[(X-\hat{X})(X-\hat{X})^T]\right| \geq \frac{1}{q[X]} - 1, \tag{6}$$

with equality if and only if X is Gaussian and $\hat{X} = E[X]$.

Proof. Following the same arguments as in [19, Th. 8.6.6],

$$\left|E[(X-\hat{X})(X-\hat{X})^T]\right| \geq \min_{\hat{X}\in\mathbb{R}^n} \left|E[(X-\hat{X})(X-\hat{X})^T]\right|$$
$$= \left|E[(X-E[X])(X-E[X])^T]\right| = |\mathrm{var}(X)|$$

and since a Guassian distribution has the greatest entropy of a given variance [19, Th. 8.6.6],

$$\left|E[(X-\hat{X})(X-\hat{X})^T]\right| \geq \frac{e^{2h[X]}}{(2\pi e)^n} = \frac{1}{q[X]} - 1. \qquad \square$$

Corollary 2. *For any 1-D continuous random variable x and any $\hat{x} \in \mathbb{R}$, the expected estimation error is lower-bounded as*

$$E[(x-\hat{x})^2] \geq \frac{1}{q[x]} - 1 \tag{7}$$

with equality if and only if x is Gaussian and $\hat{x} = E[x]$.

Proof. Use Thm. 1 with $P \in \mathbb{S}^1_{++} \implies |P| = P$. □

Remark 1. Although there is a one-to-one mapping between clarity and differential entropy (2), the primary benefits of clarity are: (I) clarity is bounded over $[0, 1]$ instead of $[-\infty, \infty]$, (II) the time derivatives, defined later in (12), are finite for all $q \in [0, 1]$. This is particularly important for perceivability, since numerical methods to solve the HJB equation, defined later in (20), require bounded values and derivatives.

B. Connection between Clarity and Coverage Control

Consider the system

$$\dot{x} = f(x, u) \tag{8}$$

where the state is $x \in \mathcal{X} \subset \mathbb{R}^n$, control input is $u \in \mathcal{U} \subset \mathbb{R}^m$.

The objective in coverage control is to design a controller $\pi : \mathcal{X} \to \mathcal{U}$ for the system (8) such that closed-loop trajectories gather information over a domain $\mathcal{D} \subset \mathcal{X}$. As in [16], let $c = c(t, p)$ denote the 'coverage level' about a point $p \in \mathcal{D}$ at time t. [16] assumes the coverage increases through a sensing function $S : \mathcal{X} \times \mathcal{D} \to \mathbb{R}_{\geq 0}$ (positive when p can be sensed from x, and 0 else), and coverage decreases at a rate $\alpha : \mathcal{D} \to \mathbb{R}_{\geq 0}$. This results in the model

$$\dot{c} = S(x, p)(1 - c) - \alpha(p)c. \tag{9}$$

In [17], [18] the α term is ignored, and a point p is said to be 'covered' if $c(t, p)$ reaches a threshold c^*.

However, given specifications on the robot, sensors, and the environment, it is not clear how to systematically define S, α, c^*. [16]–[18] resort to heuristic methods.

In many practical scenarios, measurements are assimilated using a Kalman Filter. In principle, the coverage dynamics

should reflect the information gathering mechanism, i.e., the evolution of the quality of information about the environment as it is estimated using the Kalman Filter. In deriving the clarity dynamics, (see (12)), we notice similarities with (9).

Consider the simplest scenario, where we want to estimate a scalar variable $m \in \mathbb{R}$. We assume m is a stochastic process:

$$\dot{m} = w(t), \qquad w(t) \sim \mathcal{N}(0, Q), \tag{10}$$
$$y = C(x)m + v(t), \qquad v(t) \sim \mathcal{N}(0, R(x)), \tag{11}$$

where $y \in \mathbb{R}$ is the measurement. Notice $C(x), R(x)$ are robot-state dependent, emphasizing that the quality of the measurements can depend on the robot's state. For simplicity, assume x is known. The following demonstrates the setup:

Example 2. Let x be the quadrotor's state, with position $x_{pos} \in \mathbb{R}^2$ and altitude x_{alt}. The quadrotor uses a downward facing thermal camera with half-cone angle θ to measure the ocean's temperature m at a location p. Then $C(x)$ is

$$C(x) = \begin{cases} 1, & \text{if } \|x_{pos} - p\| \leq x_{alt} \tan\theta, \\ 0, & \text{else} \end{cases}$$

and, if the measurement variance is state-independent, $R(x) = R$. The ocean temperature can change stochastically by (10).

Notice that the subsystem (10), (11) satisfies the assumptions of linear-time varying Kalman Filters [21, Ch. 4], since for any given trajectory $x(t)$, the measurement model is equivalent to $y = C(t)m + v(t)$, where $C(t) = C(x(t))$ by slight abuse of notation. Therefore, the estimate has distribution $\mathcal{N}(\mu, P)$, where μ, P evolve according to:

$$\dot{\mu} = PC(x)R(x)^{-1}(y - C(x)\mu), \quad \dot{P} = Q - \frac{C(x)^2}{R(x)}P^2.$$

Since the clarity of a scalar Gaussian is $q = 1/(1+P)$,

$$\dot{q} = \frac{\partial q}{\partial P}\dot{P} = \frac{-\dot{P}}{(1+P)^2} = \frac{-1}{(1+P)^2}\left(Q - \frac{C(x)^2}{R(x)}P^2\right)$$

and therefore the clarity dynamics are

$$\dot{q} = \frac{C(x)^2}{R(x)}(1-q)^2 - Qq^2. \tag{12}$$

Remark 2. Comparing (9) with (12), one may note that their structure is remarkably similar. Clarity/coverage increase due to the first term, and decrease due to the second. However, (12) is nonlinear wrt q. Thus, although (9) has the right intuitive characteristics to describe 'coverage', (12) *has the correct dynamics corresponding to information gathering*.

Eq. (12) yields further insight. Clarity decays at a rate $-Qq^2$, i.e., due to the environment stochasticity. As clarity increases, the rate of increase of clarity, $C(x)^2(1-q)^2/R(x)$, decreases: additional measurements have diminishing value.

Although nonlinear, (12) has closed-form solutions, since it is a scalar differential Riccati equation [22, Sec. 2.15]. For constant $C(x) = C, R(x) = R$, if $C, R, Q > 0$,

$$q(t) = q_\infty\left(1 + \frac{2\gamma_1}{\gamma_2 + \gamma_3 e^{2kQt}}\right), \tag{13}$$

where $k = C/\sqrt{QR}$, $q_\infty = k/(k+1)$, $\gamma_1 = q_\infty - q_0$, $\gamma_2 = \gamma_1(k-1)$, $\gamma_3 = (k-1)q_0 - k$.

As $t \to \infty$, clarity monotonically approaches $q_\infty < 1$: if m is stochastic with non-zero variance, and measurements have non-zero variance, perfect clarity ($q = 1$) is impossible.

Theorem 3. *Let $m \in \mathbb{R}^{n_m}$ be the environment state vector, and $y \in \mathbb{R}^q$ be the sensed outputs. Suppose the environment and measurement models are*

$$\dot{m} = Am + w(t) \qquad w(t) \sim \mathcal{N}(0, Q) \tag{14a}$$
$$y = C(x)m + v(t) \qquad v(t) \sim \mathcal{N}(0, R(x)) \tag{14b}$$

with $Q \in \mathbb{S}^{n_m}_{++}$, and $R : \mathcal{X} \to \mathbb{S}^q_{++}$. Assuming $P(t) \in \mathbb{S}^{n_m}_{++}$ for all t (see [23, Sec. 11.2]) and a prior $m \sim \mathcal{N}(\mu, P)$, then

$$\dot{P} = AP + PA^T + Q - PC(x)^T R(x)^{-1}C(x)P \tag{15}$$
$$\dot{q} = q(1-q)\left(\operatorname{tr}\left(C(x)^T R^{-1}C(x)P\right) - \operatorname{tr}\left(2A + P^{-1}Q\right)\right). \tag{16}$$

Proof. Eq. (15) is the standard covariance update for the Kalman Filter. To derive (16), notice the clarity of a multivariate Gaussian is $q = 1/(1+|P|)$. Therefore,

$$\dot{q} = -\frac{1}{(1+|P|)^2}\frac{d}{dt}(|P|)$$

Since $P \in \mathbb{S}^{n_m}_{++}$, it is invertible. Using Jacobi's formula:

$$\dot{q} = \frac{-|P|\operatorname{tr}(P^{-1}\dot{P})}{(1+|P|)^2} = q(1-q)\operatorname{tr}(-P^{-1}\dot{P})$$

since $|P|/(1+|P|)^2 = q(1-q)$. Substituting in (15), and simplifying, we arrive at (16). □

Again, we see the same structure: clarity increases at a rate $\operatorname{tr}(C(x)^T R(x)^{-1}C(x)P)$, and decreases at a rate $\operatorname{tr}(P^{-1}Q)$. Furthermore, since (15, 16) are independent of y, for trajectory planning we can use the deterministic and fully known

$$\dot{X} = \tilde{f}(X, u), \quad \dot{q} = g(X, q), \tag{17}$$

where $X = [x^T, \operatorname{vec}(P)^T]^T$ is an extended state.

III. Perceivability

In this section, we introduce the concept of *perceivability*: given a robot with certain sensing and actuation capabilities, can the robot's motion over a finite time achieve a desired level of clarity with the collected sensory data? Formally,

Definition 4. A quantity $m \in \mathbb{R}$ that evolves according to (10) is *perceivable* by the system (8, 11) with clarity dynamics[1] $g : \mathcal{X} \times [0,1] \to \mathbb{R}$, to a level $q^* \in [0,1]$ at time T from an initial state $x_0 \in \mathcal{X}$ and clarity $q_0 \in [0,1]$, if there exists a controller $\pi : [0,T] \to \mathcal{U}$ s.t. the solution to

$$\begin{bmatrix}\dot{x}\\ \dot{q}\end{bmatrix} = \begin{bmatrix}f(x,\pi(t))\\ g(x,q)\end{bmatrix}, \quad \begin{bmatrix}x(0)\\ q(0)\end{bmatrix} = \begin{bmatrix}x_0\\ q_0\end{bmatrix} \tag{18}$$

satisfies $q(T) \geq q^*$.

We define the set of initial conditions from which m is perceivable as the *perceivability domain*:

[1]When using a Kalman Filter to estimate m, g is as in (12). In general, other estimators could be used, and will lead to different expressions for g.

Definition 5. The (q^*, T)-*Perceivability Domain* of a quantity $m \in \mathbb{R}$ (that evolves according to (10)) by the system (8, 11) is the set of initial states x_0 and initial clarities q_0 such that m is perceivable to a level q^* at time T:

$$\mathcal{D}(q^*, T) = \Big\{ (x_0, q_0) : \exists \pi : [0, T] \to \mathcal{U}, \\ \dot{x} = f(x, \pi(t)),\ \dot{q} = g(x, q), \\ x(0) = x_0,\ q(0) = q_0,\ q(T) \geq q^* \Big\}. \quad (19)$$

Our key insight is that perceivability is fundamentally a question of the reachability of the augmented system (18). As with backward reachable sets, the perceivability domain can be determined by a Hamilton-Jacobi-Bellman (HJB) equation:

Theorem 4. *Let* $V : [0, T] \times \mathcal{X} \times [0, 1] \to \mathbb{R}$ *solve*

$$\frac{\partial V}{\partial t} + \max_{u \in \mathcal{U}} \left(\frac{\partial V}{\partial x} f(x, u) \right) + \frac{\partial V}{\partial q} g(x, q) = 0, \quad (20a)$$

$$V(T, x, q) = q \quad \forall x \in \mathcal{X}, q \in [0, 1]. \quad (20b)$$

Then the (q^*, T)*- perceivability domain of* $m \in \mathbb{R}$ *(that evolves according to* (10)*) by the system (8, 11) is*

$$\mathcal{D}(q^*, T) = \left\{ [x_0^T, q]^T : V(0, x_0, q_0) \geq q^* \right\}. \quad (21)$$

Proof. Let $\mathcal{L}([t, T], \mathcal{U})$ be the set of piecewise continuous functions $\pi : [t, T] \to \mathcal{U}$. Define V as the maximum clarity reachable from (t, x, q):

$$V(t, x(t), q(t)) = \max_{\pi \in \mathcal{L}([t,T],\mathcal{U})} q(T) \text{ s.t. (18)}$$

By the principle of dynamic programming, for any $\delta > 0$,

$$V(t, x(t), q(t)) = \max_{\pi \in \mathcal{L}([t,t+\delta],\mathcal{U})} V(t + \delta, x(t + \delta), q(t + \delta))$$

Using a Taylor expansion about $\delta = 0$, as $\delta \to 0$,

$$V(t, x(t), q(t)) = \max_{u \in \mathcal{U}} \Big(V(t, x(t), q(t)) + \frac{\partial V}{\partial t} \delta \\ + \frac{\partial V}{\partial x} f(x, u) \delta + \frac{\partial V}{\partial q} g(x, q) \delta \Big)$$

which simplifies to (20). □

After solving V, the optimal controller is [24, Ch. 4.2]

$$\pi(t, x, q) = \operatorname*{argmax}_{u \in \mathcal{U}} \left(\frac{\partial V}{\partial x} f(x, u) \right) \quad (22)$$

IV. Simulations and Applications[2]

A. Energy-Aware Information Gathering

This example demonstrates the diminishing value of measurements. Consider the quadrotor tasked with measuring ocean temperature. It must fly to a target location, spend T seconds collecting information, and fly back. As T increases, more measurements are made and hence greater clarity is achieved, but at an energy cost. We wish to optimize T to maximize clarity and minimize energy. We model the energy cost as $E(T) = p_0 + p_1 T$, where p_0 is the energy cost of flying to and back from the target, p_1 is the hovering power draw.

[2]Code and videos: [25]

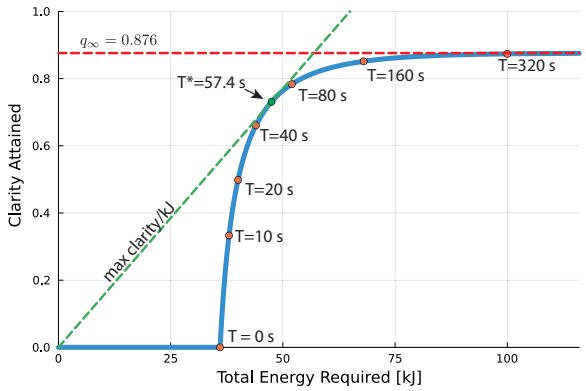

Fig. 1. Clarity gained as a function of the measurement time. First, the clarity increases rapidly. As the level of clarity approaches q_∞ (red dashed line), the rate of clarity accumulation decreases. The maximum clarity/energy ratio is (green dashed line) is achieved at $T^* = 57.4$ s. Parameters: $R = 20.0$, $Q = 0.001$, $p_0 = 36$ kJ, $p_1 = 0.2$ kW.

The pareto front of $q(T)$ against $E(T)$ is depicted in Fig. 1. The diminishing value of measurements is clearly visible, as between $T \in [160, 320]$ s, the clarity only increases by 2.6%, but increases by 49.7% for $t \in [10, 20]$ s. To maximize the clarity/energy ratio, the quadrotor should collect measurements for $T^* = 57.4$ seconds (green tangent).

B. Coverage Control based on Clarity

Next, we demonstrate how clarity can be used in ergodic coverage controller of [26]. The robot is exploring a unit square, but certain regions have a greater target clarity than others, as labelled in Fig. 2a. The challenge with ergodic controllers is defining the fraction of time spent at each position p, and uniform allocation is often used as a heuristic. Since the target clarity has been specified, we can invert (13) to determine the appropriate time allocation.

Fig. 2 compares the behaviour of three coverage controllers: (A) a greedy controller hovers at the point p with maximum $(q_T(p) - q(t, p))$ until q_T is reached, (B) the ergodic controller in [26] with a uniform target distribution, and (C) the same ergodic controller but with a target distribution based on clarity. The proposed method (C) brings the mean of $(q(t, p) - q_T(p))$ to 0 rapidly, and does not overshoot like controller B. Beyond $t = 35$, $q(t, p)$ increases further since the robot continues to explore despite most cells having reached the target clarity.

C. Perceivability and Optimal Trajectory Generation

Here we demonstrate how perceivability can be determined using (20). Consider a boat tasked with collecting information that can only be measured from the green region in Fig. 3b. To highlight the importance of actuation capabilities on perceivability, we consider two models, a single integrator:

$$\dot{x}_1 = u_1 + w_x(x),\ \dot{x}_2 = u_2 + w_y(x)$$

with $u_1, u_2 \in [-2, 2]$ m/s, and a Dubins Boat:

$$\dot{x}_1 = v \cos x_3 + w_x(x),\ \dot{x}_2 = v \sin x_3 + w_y(x),\ \dot{x}_3 = u$$

where $v = 2$ m/s, and $u \in [-1, 1]$ rad/s. For both, the sensing model is as in (12), with $C(x) = 1$ when x is in the green

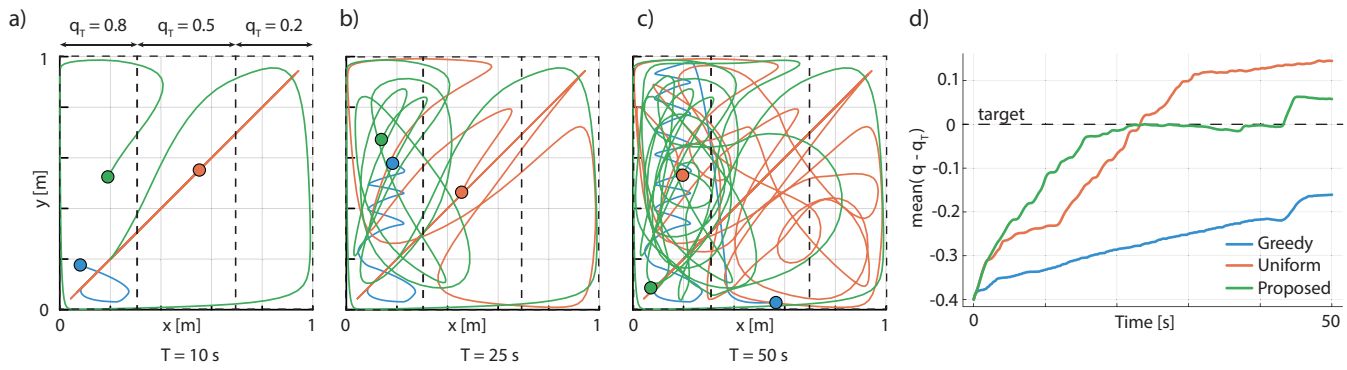

Fig. 2. Coverage Controllers. (a-c) Snapshots of three controllers exploring a square region. The target clarity $\boldsymbol{q_T(p)}$ is different in different regions as labelled in (a). (d) Plot of the mean$(\boldsymbol{q(t,p) - q_T(p)})$ against $\boldsymbol{t}$ for each controller. Notice that using the proposed method, the mean clarity error is close to 0 for $\boldsymbol{t \in [20 - 35]}$ seconds, and only increases later, when the entire region has higher clarity than the targets specified.

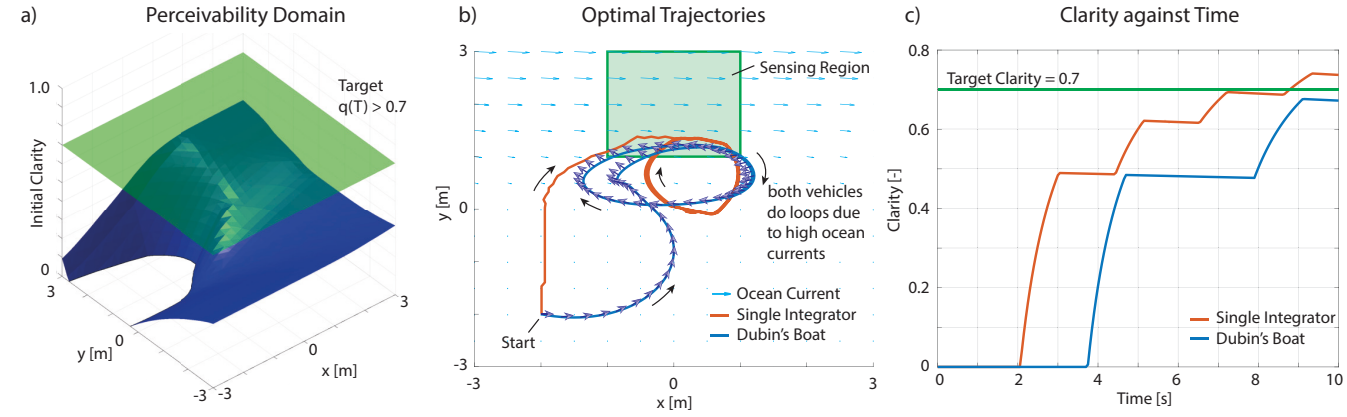

Fig. 3. Perceivability and Optimal Trajectories. (a) The $(\boldsymbol{q^*, T})$-Perceivability Domain (states above blue surface) for single integrator using $\boldsymbol{q^* = 0.7, T = 10.0}$ sec. (b) Optimal trajectories for the single integrator (orange) and the Dubins boat (blue) from the same initial conditions. The heading of Dubins boat is shown with blue arrows. Due to the high ocean currents in the sensing region, both vehicles make multiple passes through the sensing region to accumulate clarity. (c) Plot of clarity against time for both vehicles. Since the single integrator is more maneuverable than the Dubins boat, the environment is perceivable to a level 0.7 in time 10 seconds for the single integrator but not for the Dubin's boat.

square and 0 elsewhere, $R(x) = 1.0$, $Q = 0.001$. The ocean current is $w_x(x) = \max(0, 3x_2), w_y(x) = -0.5$ m/s. Thus, neither vehicle has sufficient control authority to remain within the sensing range indefinitely.

To determine the perceivability domain, the backwards reachability set of (18) is computed using [27], [28] (Fig. 3a). The optimal controller (22) drives both vehicles from the same initial condition (Fig. 3b). Due to the current, both vehicles need to do loops to acquire clarity. The single integrator (Fig. 3c) is able to reach $q(T) \geq q^*$, while Dubins boat is not. Despite having the same sensing capabilities, the perceivability is different due to different actuation capabilities.

Computing the 10-second perceivability domain took 450 seconds on a Macboook Pro (i9, 2.3GHz, 16GB). While prohibitively slow for online applications, V can be precomputed offline. Future work will explore faster trajectory design techniques, akin to RIG [1], or CBFs, as demonstrated next.

D. CBF-based Trajectory Generation

Here we demonstrate how Lyapunov methods can be used to efficiently design controllers that maintain an information constraint, avoiding the need to numerically solve the HJB equation. Consider a 6D planar quadrotor system [29],

$$\ddot{x}_1 = u_1 \sin x_3/m,\ \ddot{x}_2 = u_1 \cos x_3/m - g,\ \ddot{x}_3 = u_2/J$$

where x_1, x_2 is the position of the quadrotor in the vertical plane, and x_3 is the pitch angle. m, g, J are the mass, acceleration due to gravity, and moment of inertia. The quadrotor is attempting a precision landing, using onboard sensors to determine the landing spot x_f. Given an estimate $\hat{x}_f$, an optimal control problem (OCP) can be solved to reach $\hat{x}_f$. However, since $\hat{x}_f$ is estimated online, we must ensure $\hat{x}_f$ is accurate before approaching it. This can be encoded as $\sigma \leq x_2/2$, which ensures that σ, the standard deviation of the estimated landing site is less than half the altitude, x_2. A constrained OCP can be defined, but is numerically difficult to solve since there are 7 state and 2 input dimensions.[3]

Instead, Lyapunov methods can be used to maintain the constraint. Using $\sigma^2 = 1/q - 1$, the safe set is

$$\mathcal{S} = \{[x^T, q]^T : h(x, q) = q - 4/(4 + x_2^2) \geq 0\}$$

where h is a CBF of relative degree 2 [30]. Fig. 4 compares the trajectories with and without the CBF-QP controller [31]. With the CBF-QP controller the quadrotor slows down to ensure high quality of information. Each iteration of the controller takes about 1 ms, significantly faster than HJB methods. This illustrates that by framing problems of information-based

[3]It took 480 s to compute the 0.05 s horizon value function on a coarse grid. Over a finer grid, the RAM usage exceeded 60GB and MATLAB crashed.

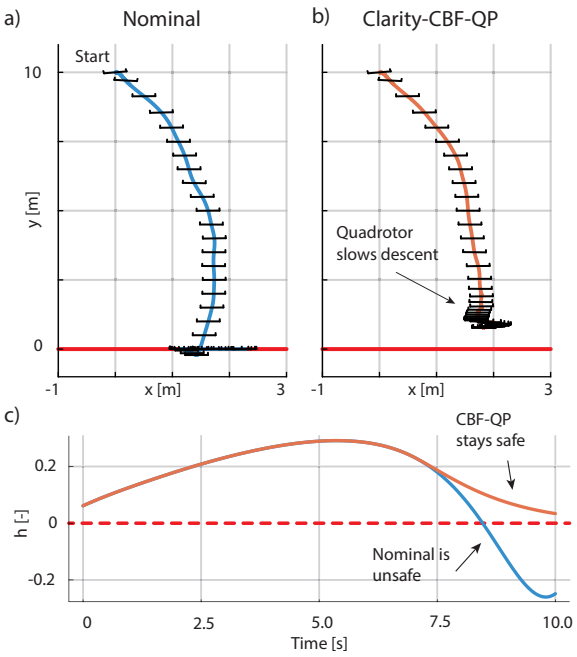

Fig. 4. Precision landing of a planar quadrotor. (a) In the nominal controller, the quad descends rapidly and misses the target. (b) Using the clarity based CBF-QP controller, the quad descends slowly. (c) Plot of h against t, showing the CBF-QP keeps the system safe.

control using clarity/perceivability, Lyapunov methods can be used to design controllers to maximize (or in this case maintain) the quality of information gathered by a system.

V. Conclusion

The primary purpose of this paper is to introduce perceivability, the ability of a robotic system to obtain information about the environment contingent on its actuation capabilities, its sensing capabilities, the environment's dynamics. As a metric for information, we introduce clarity, a bounded rescaling of differential entropy that takes values in $[0, 1]$. We have shown how perceivability is linked to a reachability problem of an augmented state, and through HJB equations, simultaneously determine a system's perceivability and the optimal control policy to maximize the final clarity. By using clarity, the HJB-based algorithms can be evaluated numerically, since (A) the range of the information state is bounded, and (B) the clarity dynamics have finite derivative. In the simulations, we demonstrate other ways that the clarity and perceivability can be used, from minimizing the energy cost, or designing CBF-QP controllers to maintain a desired level of information.

In this introductory paper, we considered stochastic environments and measurement models, but deterministic robot dynamics. The important case of stochastic robot dynamics will be studied in the future. We also intend to investigate a potential connection with data-informativity [13]: perhaps data-informative trajectories can be designed using perceivability, to improve data-driven system identification.

References

[1] G. A. Hollinger and G. S. Sukhatme, "Sampling-based motion planning for robotic information gathering.," in *Robotics: Science and Systems*, vol. 3, pp. 1–8, 2013.

[2] H. Touchette and S. Lloyd, "Information-theoretic approach to the study of control systems," *Physica A: Statistical Mechanics and its Applications*, vol. 331, no. 1-2, pp. 140–172, 2004.

[3] J.-C. Delvenne and H. Sandberg, "Towards a thermodynamics of control: Entropy, Energy and Kalman filtering," in *IEEE CDC*, pp. 3109–3114, 2013.

[4] N. Cao, K. H. Low, and J. M. Dolan, "Multi-robot informative path planning for active sensing of environmental phenomena: A tale of two algorithms," *arXiv preprint arXiv:1302.0723*, 2013.

[5] B. Moon, S. Chatterjee, and S. Scherer, "Tigris: An informed sampling-based algorithm for informative path planning," in *IEEE IROS*, pp. 5760–5766, 2022.

[6] Z. Zhang and D. Scaramuzza, "Beyond point clouds: Fisher information field for active visual localization," in *IEEE ICRA*, pp. 5986–5992, 2019.

[7] C. Cai and S. Ferrari, "Information-driven sensor path planning by approximate cell decomposition," *IEEE TSMC*, vol. 39, no. 3, pp. 672–689, 2009.

[8] B. Zhou, Y. Zhang, X. Chen, and S. Shen, "FUEL: Fast UAV exploration using incremental frontier structure and hierarchical planning," *IEEE RAL*, vol. 6, no. 2, pp. 779–786, 2021.

[9] J. Cortes, S. Martinez, T. Karatas, and F. Bullo, "Coverage control for mobile sensing networks," *IEEE T-RO*, vol. 20, no. 2, pp. 243–255, 2004.

[10] B. Jiang, Z. Sun, and B. D. Anderson, "Higher order Voronoi based mobile coverage control," in *IEEE ACC*, pp. 1457–1462, 2015.

[11] M. Popović, T. Vidal-Calleja, J. J. Chung, J. Nieto, and R. Siegwart, "Informative path planning for active field mapping under localization uncertainty," in *IEEE ICRA*, pp. 10751–10757, 2020.

[12] R. Marchant and F. Ramos, "Bayesian optimisation for informative continuous path planning," in *IEEE ICRA*, pp. 6136–6143, 2014.

[13] H. J. Van Waarde, J. Eising, H. L. Trentelman, and M. K. Camlibel, "Data informativity: a new perspective on data-driven analysis and control," *IEEE TAC*, vol. 65, no. 11, pp. 4753–4768, 2020.

[14] A. Bry and N. Roy, "Rapidly-exploring random belief trees for motion planning under uncertainty," in *IEEE ICRA*, pp. 723–730, 2011.

[15] C. Xiao and J. Wachs, "Nonmyopic informative path planning based on global kriging variance minimization," *IEEE RAL*, vol. 7, no. 2, pp. 1768–1775, 2022.

[16] B. Haydon, K. D. Mishra, P. Keyantuo, D. Panagou, F. Chow, S. Moura, and C. Vermillion, "Dynamic coverage meets regret: Unifying two control performance measures for mobile agents in spatiotemporally varying environments," in *IEEE CDC*, pp. 521–526, 2021.

[17] D. Panagou, D. M. Stipanović, and P. G. Voulgaris, "Distributed dynamic coverage and avoidance control under anisotropic sensing," *IEEE TCNS*, vol. 4, no. 4, pp. 850–862, 2016.

[18] W. Bentz and D. Panagou, "A hybrid approach to persistent coverage in stochastic environments," *Automatica*, vol. 109, p. 108554, 2019.

[19] M. Thomas and A. T. Joy, *Elements of information theory*. Wiley-Interscience, 2006.

[20] C. E. Shannon, "A mathematical theory of communication," *The Bell system technical journal*, vol. 27, no. 3, pp. 379–423, 1948.

[21] A. Gelb *et al.*, *Applied optimal estimation*. MIT press, 1974.

[22] E. L. Ince, *Ordinary differential equations*. Longmans, GReen and Company Limited, 1927.

[23] H. K. Khalil, *Nonlinear control*, vol. 406. Pearson New York, 2015.

[24] A. E. Bryson, *Applied optimal control: optimization, estimation and control*. CRC Press, 1975.

[25] D. R. Agrawal, "Github repo." `https://github.com/dev10110/Clarity-and-Perceivability`, 2023.

[26] G. Mathew and I. Mezić, "Metrics for ergodicity and design of ergodic dynamics for multi-agent systems," *Physica D: Nonlinear Phenomena*, vol. 240, no. 4-5, pp. 432–442, 2011.

[27] I. M. Mitchell and J. A. Templeton, "A toolbox of Hamilton-Jacobi solvers for analysis of nondeterministic continuous and hybrid systems," in *Hybrid Systems: Computation and Control.*, pp. 480–494, Springer, 2005.

[28] S. Bansal, M. Chen, S. Herbert, and C. J. Tomlin, "Hamilton-Jacobi reachability: A brief overview and recent advances," in *IEEE CDC*, pp. 2242–2253, 2017.

[29] D. R. Agrawal and D. Panagou, "Safe and robust observer-controller synthesis using control barrier functions," *IEEE L-CSS*, vol. 7, pp. 127–132, 2022.

[30] A. D. Ames, X. Xu, J. W. Grizzle, and P. Tabuada, "Control barrier function based quadratic programs for safety critical systems," *IEEE TAC*, vol. 62, no. 8, pp. 3861–3876, 2016.

[31] W. Xiao and C. Belta, "Control barrier functions for systems with high relative degree," in *IEEE CDC*, pp. 474–479, 2019.